Pergamon

Int. Comm. Heat Mass Transfer, Vol. 26, No. 7, pp. 965–974, 1999

0735-1933/99/$–see front matter

PII S0735-1933(99)00086-X

RISE CHARACTERISTICS OF GAS BUBBLES IN A 2D RECTANGULAR COLUMN: VOF SIMULATIONS VS EXPERIMENTS

R. Krishna and J.M. van Baten
Department of Chemical Engineering, University of Amsterdam
Nieuwe Achtergracht 166, 1018 WV Amsterdam, The Netherlands

(Communicated by J.W. Rose and A. Briggs)

ABSTRACT

About five centuries ago, Leonardo da Vinci described the sinuous motion of gas bubbles rising in water. We have attempted to simulate the rise trajectories of bubbles of 4, 5, 7, 8, 9, 12 and 20 mm in diameter rising in a 2D rectangular column filled with water. The simulations were carried out using the volume-of-fluid (VOF) technique developed by Hirt and Nichols (*J. Computational Physics.*, **39**, 201-225 (1981)). To solve the Navier-Stokes equations of motion we used a commercial solver, CFX 4.1c of AEA Technology, UK. We developed our own bubble-tracking algorithm to capture "sinuous" bubble motions. The 4 and 5 mm bubbles show large lateral motions observed by Da Vinci. The 7,8 and 9 mm bubble behave like jellyfish. The 12 mm bubble flaps its wings like a bird. The extent of lateral motion of the bubbles decreases with increasing bubble size. Bubbles larger than 20 mm in size assume a spherical cap form and simulations of the rise characteristics match experiments exactly. VOF simulations are powerful tools for *a priori* determination of the morphology and rise characteristics of bubbles rising in a liquid. Bubble-bubble interactions are also properly modelled by the VOF technique. © 1999 Elsevier Science Ltd

Introduction

In many branches of engineering it is important to be able to describe the motion of gas bubbles in a liquid. The rise characteristics of a bubble are strongly dependent on the bubble size. For the air-water system, bubbles in the 2 – 12 mm size range show complex rise characteristics. The first recorded observation of these rise characteristics is to be found in the writings of Leonardo da Vinci. About five centuries ago, Da Vinci summarised his observations on the motion of air bubbles in a liquid in the following manner. "*The air that submerged itself with the water which percussed upon the other water, returns to the air, penetrating the water in sinuous movement, changing its substance into a great number of forms. And this happens because "the light thing cannot remain under the heavy"; rather it is continuously pressed by the part of the liquid which rests upon it; and because the water that stands there perpendicular is more powerful than the other in its decent, this water is always driven away by the part of the water that form its coverings, and so moves more continually sideways where it is less heavy and in*

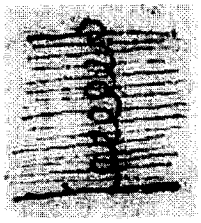

FIG. 1
Sinuous motion of a gas bubble in a liquid. Drawing by Leonardo da Vinci. The original text containing his writings are available on CD-ROM, Leonardo da Vinci, Corbis Corporation, 1996.

consequence offers less resistance, according to the 5th [proposition] of the 2nd [Book]; and because this "has to make its movement by the shortest way", it never spreads itself out from its path except to the extent to which it avoids the water which covers it above." Leonardo da Vinci's sketch of the bubble rise trajectory in water is reproduced in Fig. 1. Five hundred years on, we have attempted to simulate the motion of single gas bubbles in a liquid using the volume-of-fluid (VOF) technique developed by Hirt and Nichols [1]. Our objective is to see how far the VOF technique can be used for *a priori* simulations of bubble trajectories. A further objective of this paper is to examine bubble-bubble interactions in swarms using the VOF technique.

VOF Simulation Method and Results

The VOF model (Hirt and Nichols [1], Delnoij et al. [2]; Tomiyama et al. [3,4]) resolves the transient motion of the gas and liquid phases using the Navier-Stokes equations, and accounts for the topology changes of the gas-liquid interface induced by the relative motion between the dispersed gas bubble and the surrounding liquid. The finite-difference VOF model uses a donor-acceptor algorithm, originally developed by Hirt and Nichols [1], to obtain, and maintain, an accurate and sharp representation of the gas-liquid interface. The VOF method defines a fractional volume or "colour" function $c(\mathbf{x},t)$ that indicates the fraction of the computational cell filled with liquid. The colour function varies between 0, if the cell is completely occupied by gas, and 1, if the cell consists only of the liquid phase. The location of the bubble interface is tracked in time by solving a balance equation for this function:

$$\frac{\partial c(\mathbf{x},t)}{\partial t} + \nabla \bullet \left(\mathbf{u} c(x,t)\right) = 0 \qquad (1)$$

The liquid and gas velocities are assumed to equilibrate over a very small distance and essentially $\mathbf{u}_k = \mathbf{u}$ for k = L, G at the bubble interface. The mass and momentum conservation equations can be considered to be homogenous:

TABLE 1

Results of two-dimensional VOF simulations in Cartesian geometry. In all cases the gas phase was air (ρ_G = 1.29 kg m^{-3}, μ_G = 1.7×10^{-5} Pa s) and the liquid was water (ρ_L = 998; μ_L = 10^{-3} ; σ = 0.072 N/m)

Bubble diameter, d_b /[m]	Column diameter, D_T/[m]	Grid size, Δx (= Δz) /[mm]	Time step, Δt /[s]	Rise velocity, V_b/[m s^{-1}]
0.004	0.025	0.125	0.0003	0.1054
0.005	0.025	0.125	0.0001	0.1195
0.007	0.025	0.125	0.0002	0.1095
0.008	0.025	0.2	0.0005	0.1123
0.009	0.04	0.16	0.0003	0.1315
0.012	0.04	0.16	0.0003	0.1316
0.020	0.4	1	0.0004	0.277
0.0203	0.6	1	0.0004	0.275
0.021	0.051	1	0.0004	0.16
0.031	0.3	1	0.0004	0.317
0.033	0.051	1	0.0004	0.163
0.0359	0.051	1	0.0004	0.1605
0.046	0.051	1	0.0004	0.168
0.033	0.1	1	0.0004	0.2235
Swarm of eight 5 mm bubbles	0.025	0.125	0.0001	

$$\nabla \bullet (\rho \mathbf{u}) = 0 \tag{2}$$

$$\frac{\partial \rho \mathbf{u}}{\partial t} + \nabla \bullet (\rho \mathbf{u}\mathbf{u}) = -\nabla p - \nabla \bullet \tau + \rho \mathbf{g} + \mathbf{F}_{sf} \tag{3}$$

where p is the pressure, τ is the viscous stress tensor, $\mathbf{g}$ is the gravitational force. The density and viscosity used in eqs (2) and (3) are calculated from

$$\rho = \varepsilon_L \rho_L + \varepsilon_G \rho_G; \quad \mu = \varepsilon_L \mu_L + \varepsilon_G \mu_G \tag{4}$$

where ε_k denotes the volume fraction of the phase k = L,G. The continuum surface force model, originally proposed by Brackbill et al. [5], is used to model the force due to surface tension acting on the

gas-liquid interface. In this model the surface tension is modelled as a body force $\mathbf{F}_{sf}$, that is non-zero only at the bubble interface and is given by the gradient of the colour function

$$\mathbf{F}_{sf} = \sigma \kappa(\mathbf{x}) \nabla c(\mathbf{x},t) \tag{5}$$

where $\kappa(\mathbf{x})$ is the local mean curvature of the bubble interface:

$$\kappa(\mathbf{x},t) = -\nabla \bullet \left(\mathbf{n}/|\mathbf{n}|\right) \tag{6}$$

where $\mathbf{n}$ is the vector normal to the bubble interface

$$\mathbf{n} = \nabla c(\mathbf{x},t) \tag{7}$$

The set of equations (1) – (7) were solved using the commercial flow solver CFX 4.1c of AEA Technology, Harwell, UK. This package is a finite volume solver, using body-fitted grids. The grids are non-staggered and all variables are evaluated at the cell centres. An improved version of the Rhie-Chow algorithm [6] was used to calculate the velocity at the cell faces. The pressure-velocity coupling is obtained using the SIMPLEC algorithm (Van Doormal and Raithby [7]).

All simulations reported here were carried out in a rectangular column using a uniform 2D Cartesian co-ordinate grid; details are given in Table 1. A uniform grid was used. The front of the 2D rectangular grid is formed by the x-z – plane. The front and rear faces of the column are modelled as symmetry planes. At the two walls, the no-slip boundary condition is imposed. The column is modelled as an open system, so the pressure in the gas space above the initial liquid column is equal to the ambient pressure (101.325 kPa). For the convective terms in the equations hybrid differencing was used. Upwind differencing was used for the time integration. The time step used in the simulations were usually 0.0004 s or smaller. To counteract excessive smearing of the liquid-gas interface by numerical diffusion, a surface sharpening routine was invoked. This routine identifies gas and liquid on the "wrong" side of the interface, and moves it back to the correct side, while conserving volume of the respective phases. In order to avoid "dissolution" of the bubble due to surface sharpening we found it necessary to ensure that each bubble area encompassed a few hundred cells. For simulations of bubble sizes smaller than 12 mm, we found that the rich dynamic features could be captured only by allowing at least 800 grid cells per bubble cross-section. This constraint resulted in grid sizes as small as 0.125 mm for the smallest bubble size we could simulate with adequate accuracy; see Table 1. For simulation of the rise of spherical cap bubbles, typically found with sizes above 17 mm, a grid size of 1 mm was found to be adequately small; in this case the number of grid cells per bubble cross-section was in excess of 300. For all simulations reported here a bubble neither gained nor lost more than about 10% area during its rise.

All simulations were carried out using the parallel version of CFX 4.1c running on a Silicon Graphics Power Challenge machine with six R8000 processors. To give an indication of the required CPU time, the simulation of the rise of a 7 mm diameter bubble for 0.75 s in a column of 0.025 m width and 0.09 m height, involving 144000 grid cells, required about two weeks.

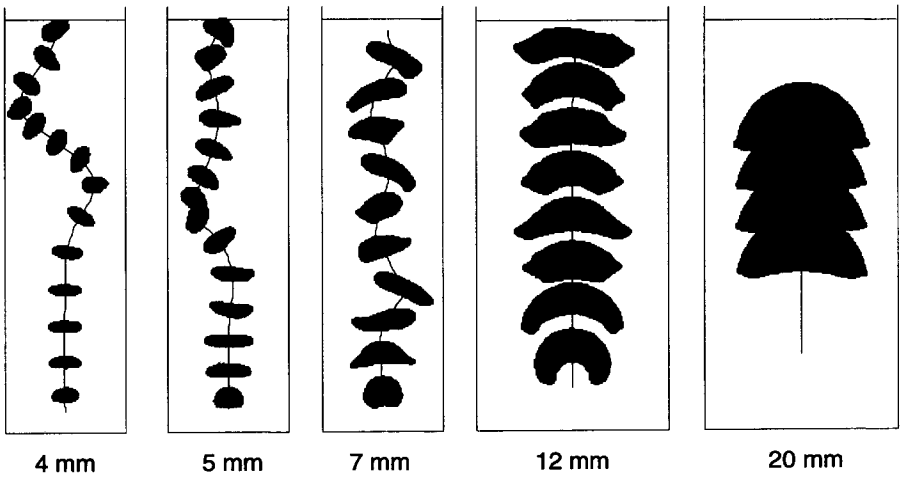

FIG. 2
Rise trajectories of bubbles of 4,5,7,12 and 20 mm diameter in a column of water.

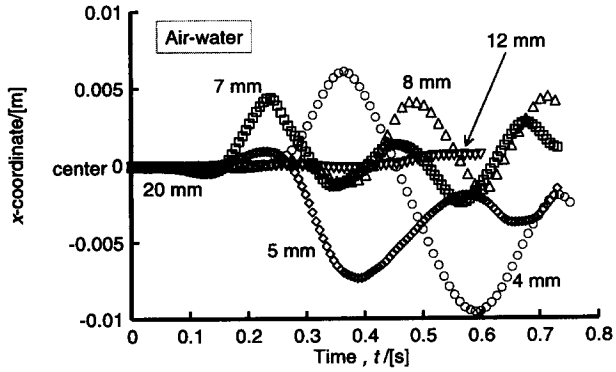

FIG. 3
x-coordinates of the rise trajectories of 4,5,7,8,12 and 20 mm air bubbles in 2D liquid column.

Snapshots of typical bubble trajectories obtained are shown in Fig. 2. The 4 and 5 mm bubbles show meandering trajectories, alluded to by Da Vinci. As the bubble size increases the amplitude of these excursions in the x-directions decrease; see Fig. 3. The 4 and 5 mm bubbles meander up the column with large lateral movements, in conformity with the observations of Leonardo da Vinci. The 7 mm bubble oscillates from side to side when moving up the column. The 8 and 9 mm bubbles behave like jellyfish. The 12 mm bubble flaps its "wings" like a bird. The 20 mm bubble assumes a spherical cap form and rises vertically up the column. These rich dynamic features can be viewed by looking at the animations of the simulations that can be found on our web site *http://ct-cr4.chem.uva.nl/single_bubble/*. The rise velocity of bubbles in the 3 - 10 mm range are virtually independent of the bubble size, in conformity with experimental evidence (Clift et al. [8]; Fan and Tsuchiya [9]).

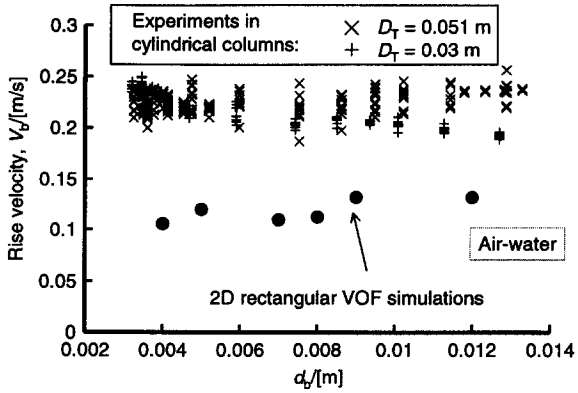

FIG. 4
Comparison of the rise velocities determined from 2D VOF simulations with experimental data in cylindrical columns.

The rise velocity of spherical cap bubbles, which meet with the criterion Eö >40, is found to be a unique function of the ratio of the bubble diameter to the column diameter, d_b/D_T. The Froude number defined as $V_b/\sqrt{(g\ d_b)}$ is plotted against d_b/D_T in Fig. 4 for the VOF simulations of bubbles larger than 20 mm; these bubbles meet with the criterion that the Eötvös number should be greater than 40 (Clift et al. [8]) in order to obtain spherical cap bubbles. The rise of the spherical cap bubbles is in inviscid flow that means that the liquid phase viscosity does not have an effect on the rise characteristics. Figure 5 compares the Froude number, $V_b/\sqrt{(g\ d_b)}$, calculated from the simulation results with the experimental data obtained in a 2D rectangular column (0.3 m wide, 3 m height and 5 mm deep) with the system air-water. The agreement between the simulations and experiment is excellent, leading us to conclude that VOF simulations can be used for *a priori* calculation of the rise velocity of spherical cap bubbles. This could be a powerful investigative tool because it is easier in a VOF simulation to change the physical properties of the gas and liquid phases than in experiments. For example, the liquid viscosity can be changed while keeping the surface tension constant.

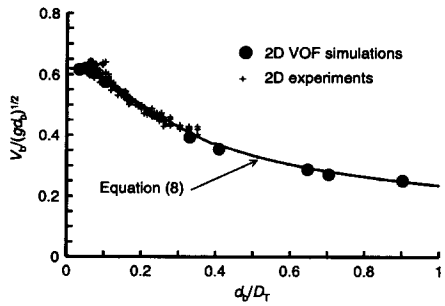

FIG. 5
Scale effects on the rise velocity of spherical cap bubbles in 2D column. Eö >40 for these runs.

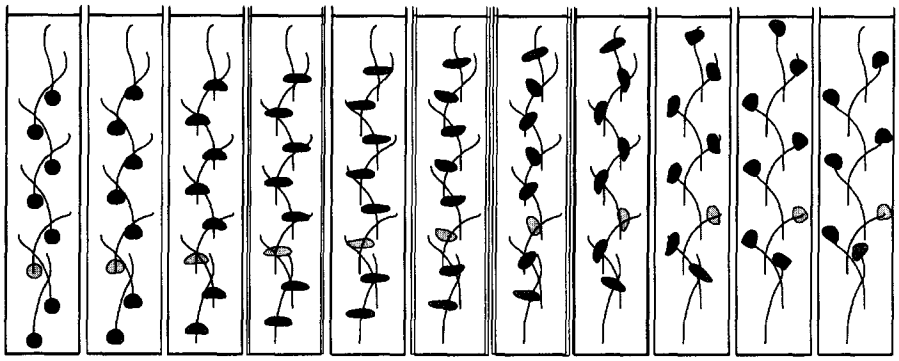

FIG. 6
Rise trajectories of a swarm of 5 mm bubbles, eight in number, in a column of liquid.

Combining the experimental results with VOF simulations allows us to set up the following set of equations to describe the rise velocity of spherical cap bubbles in a 2D rectangular column.

$$V_b = 0.62\sqrt{gd_b} \qquad \text{for } d_b/D_T < 0.07 \tag{8a}$$

$$V_b = 0.62\sqrt{gd_b}\left(1.1\exp(-1.55\,d_b/D_T)\right) \qquad \text{for } 0.07 < d_b/D_T < 0.4 \tag{8b}$$

$$V_b = 0.236\sqrt{gD_T} \qquad \text{for } d_b/D_T > 0.4 \tag{8c}$$

Equations (8) may be regarded as the two-dimensional analogue of the Collins [10] relations.

Bubble-Bubble Interactions in Swarms

There is a significant difference between the behaviour of a swarm of "small" bubbles, typically smaller than say 10 mm and a swarm of "large" bubbles, typically larger than 10 mm in size. To illustrate this we carried out a simulation a swarm of 8 bubbles, each of 5 mm size. In order to ensure convergence of this simulation it was necessary to use an extremely small time step of 0.0001 s. The lines in the various snapshots shown in Fig. 6 at various time intervals indicate the rise trajectories of each bubble in the swarm. The bubbles try to "avoid" each other as they move upwards. This is clearly evident from the animation in our web site *http://ct-cr4.chem.uva.nl/single_bubble/*, which gives further details. This "hindrance" effect is described by Richardson-Zaki relationship for rise of a swarm of gas bubbles in a liquid [11].

The VOF technique was also used to study the bubble-bubble interactions in a swarm of large bubbles (larger than 10 mm) for air-water system in a rectangular 2D column of 0.3 m width. In sharp contrast to the behaviour of small bubbles, as seen above, large bubbles are seen to suffer frequent coalescence and break-up. The animations of these simulations, along with details of the simulations are to be found on our web site *http://ct-cr4.chem.uva.nl/breakup/*. Some snapshots of these simulations are

shown in Fig. 7 illustrating the coalescence and break-up processes. By a frame-by-frame analysis we determined the death rate of bubbles in various class ranges; the death rates found from VOF simulations match quite well with measurements we had carried out earlier for the air-water system using video imaging techniques in a column of identical dimensions as used in the simulations (De Swart et al. [12,13]); see Fig. 8.

Concluding Remarks

- VOF simulations with gas-liquid systems could be used as an investigative tool for studying bubble rise and bubble-bubble interactions in gas-liquid bubble columns.
- 2D VOF simulations of bubbles in the 4 – 12 mm diameter range reveal the rich dynamic features of bubble rise but are not able to provide quantitative agreement with experimental data in cylindrical columns.
- For spherical cap bubbles (meeting with the criterion Eö > 40) the rise velocity is a significant function of the ratio d_b/D_T. VOF simulations are in excellent agreement with experimental data.
- A swarm of small bubbles tend to avoid each other. This results in a hindrance effect, described by the Richardson-Zaki relation [11].
- Large bubbles in a swarm suffer frequent coalescence and break-up. The break-up rates from VOF simulations match experiments reasonably well.

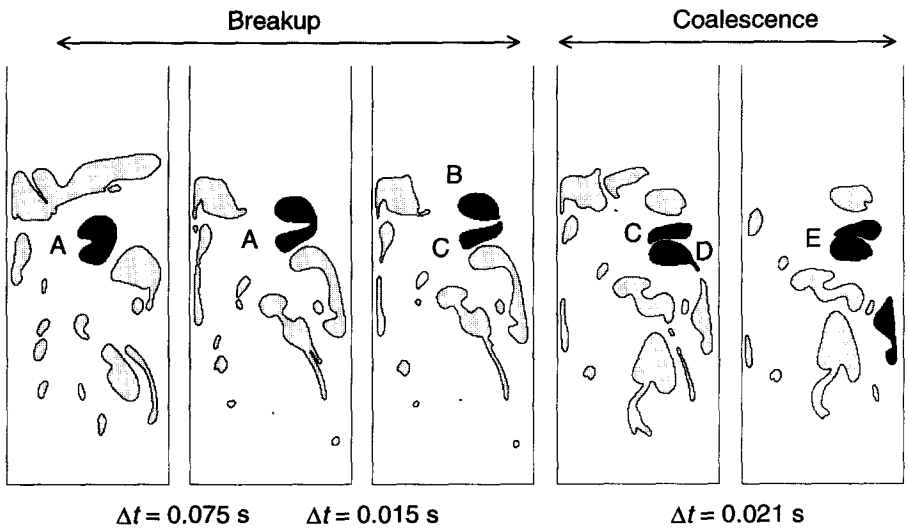

FIG. 7
VOF simulations of coalescence and breakup in a 2D column of 0.3 m width.

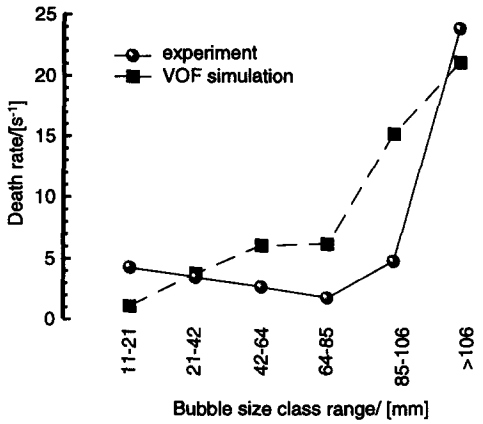

FIG. 8
Death rate of large bubbles according to various size classes. Comparison of results from VOF simulations with experimental results of De Swart [12].

Nomenclature

$c(\mathbf{x},t)$	colour function, -
d_b	bubble diameter, m
D_T	column diameter, m
Eö	Eötvös number, $g(\rho_L - \rho_G)d_b^2/\sigma$
$\mathbf{F}_{sf}$	surface tension force, N m^{-3}
g	acceleration due to gravity, 9.81 m s^{-2}
$\mathbf{n}$	vector normal to the interface
p	pressure, N m^{-2}
t	time, s
$\mathbf{u}$	velocity vector, m s^{-1}
V_b	rise velocity of the bubble, m s^{-1}
x	x-coordinate (horizontal), m
Δx	grid size in the horizontal (x-) direction, m
$\mathbf{x}$	position vector, m
z	distance coordinate along height of cylindrical column, m
Δz	grid size in the vertical (z-) direction, m
ε	volume fraction of phase, -
$\kappa(\mathbf{x})$	curvature of bubble interface, -
μ	viscosity of phase, Pa s

ρ	density of phase, kg m^{-3}
σ	surface tension of liquid phase, N m^{-1}
τ	viscous stress tensor, N m^{-2}

Subscripts

b	referring to bubble
G	referring to gas phase
k	referring to either gas or liquid phase
L	referring to liquid phase
T	tower or column

Operators

∇	gradient (Nabla) operator
$\nabla\bullet$	divergence

References

1. C.W. Hirt and B.D. Nichols, *J. Computational Physics*, **39**, 201 (1981).
2. E. Delnoij, J.A.M.Kuipers and W.P.M. van Swaaij, *Chem.Eng.Sci.*, **52**, 3623 (1997).
3. A. Tomiyama, I. Zun, A. Sou and T. Sakaguchi, *Nuclear Engineering and Design*, **141**, 69 (1993).
4. A. Tomiyama, A. Sou, H. Minagawa and T. Sakaguchi, *JSME International Journal, Series B*, **36**, 51(1993).
5. J.U. Brackbill, D.B. Kothe and C. Zemarch, *J. Comput. Physics*, **100**, 335 (1992).
6. C.M. Rhie and W.L. Chow, *AIAA Journal*, **21**, 1525 (1983).
7. J. Van Doormal, and G.D. Raithby, *Numer. Heat Transfer*, **7**, 147 (1984).
8. R. Clift, J.R. Grace and M.E. Weber, Bubbles, drops and particles. Academic Press, San Diego (1978).
9. L.S. Fan and K. Tsuchiya, Bubble wake dynamics in liquids and liquid-solid suspensions, Butterworth Heinemann, Boston (1990).
10. R. Collins, *J. Fluid Mech.*, **28**, 97 (1967).
11. G.B. Wallis, One-dimensional two-phase flow. McGraw-Hill, New York (1969).
12. J.W.A. de Swart, Scale up of a Fischer Tropsch slurry reactor, Ph.D. thesis in Chemical Engineering, University of Amsterdam, Amsterdam (1996).
13. J.W.A. de Swart, R.E. van Vliet and R. Krishna, *Chem.Eng.Sci.*, **51**, 4619 (1996).

Received May 3, 1999